Applied Materials Today 15 (2019) 335–342

Contents lists available at ScienceDirect

Applied Materials Today

journal homepage: www.elsevier.com/locate/apmt

Mildly oxidized SWCNT as new potential support membrane material for effective H_2/CO_2 separation

Marie Boháčová[a,b], Kateřina Zetková[a], Petr Knotek[c], Daniel Bouša[b], Karel Friess[d], Petr Číhal[d], Marek Lanč[d], Zdeněk Hrdlička[e], Zdeněk Sofer[b,*]

[a] Synpo, a.s., S. K. Neumanna 1316, Pardubice 532 07, Czech Republic
[b] Department of Inorganic Chemistry, University of Chemistry and Technology Prague, Technicka 5, 166 28 Prague 6, Czech Republic
[c] Department of General and Inorganic Chemistry, University of Pardubice, Studentska 95, 532 10 Pardubice, Czech Republic
[d] Department of Physical Chemistry, University of Chemistry and Technology Prague, Technicka 5, 166 28 Prague 6, Czech Republic
[e] Department of Polymer Chemistry, University of Chemistry and Technology Prague, Technicka 5, 166 28 Prague 6, Czech Republic

ARTICLE INFO

Article history:
Received 1 January 2019
Received in revised form 14 February 2019
Accepted 20 February 2019

Keywords:
Membrane
Gas separation
Carbon nanotubes
Carbon dioxide
Hydrogen

ABSTRACT

We demonstrate challenging material properties of flat free-standing chemically modified single wall carbon nanotube (SWCNT) sheets potentially usable as new support materials for gas separation composite membranes. Carbon nanotube samples in bare and oxidized forms were assembled into buckypaper by a vacuum filtration from SWCNT colloidal suspension. The fundamental structure, composition and mechanical properties were examined via SEM, EDS, AFM, XPS, Raman spectroscopy and dynamical mechanical analysis. Gas permeability was determined by the fixed-volume pressure-increase permeation method at 25 °C and 1 bar feed overpressure. The mild SWCNT oxidation caused substantial structural rearrangement of buckypaper with significant impact on its properties. Determined partial opening of nanotubes and the introduction of oxygen-containing species decreased the initial extremely-high H_2 permeability from circa 20 million (bare) to almost 5 million barrers while the ideal H_2/CO_2 selectivity α increased from almost non-selective 1.1 (bare) to 3.5 for the oxidized sample. Furthermore, oxidized form exhibited 2 times lower tensile strength but 2.5 times higher ductility. Such behavior indicates improved mechanical properties of oxidized samples that can undergo significant plastic deformation before the rupture. Determined features make mildly oxidized SWCNT buckypapers potentially attractive as new robust and tunable membrane support material for highly effective hydrogen separation.

1. Introduction

Generally, the composite or hybrid gas separation membranes [1–4] consist at least of two different materials. The top, dense, and thin selective layer (skin) is usually supported by the porous, thick sublayer with the appropriate inner structure. The support materials should exhibit a minor or negligible resistance to the passage of gas while at the same time should offer adequate chemical and mechanical stability, high porosity, sufficient flexibility, long-term stability and suitable interfacial structure and roughness. Such layered arrangement offers many advantages, including the possibility (i) to optimize membrane performance by independent tailoring each layer properties according to their different functions and (ii) to reduce the overall transport resistance by using highly permeable supports and extremely thin selective top-layers [1]. However, small failures of porous supports can significantly affect the properties of the top layer and, consequently, degrade the overall membrane performance [1]. The most commonly used techniques (dip-coating, interfacial polymerization, spin-coating and solution-casting) are currently used to prepare very thin (ultrathin) polymer membranes while chemical vapour deposition technique has been mainly used for the deposition of inorganic thin films [1,4]. Flexible polymeric supports (nylon, polyacrylonitrile, polyimide, polyether–ether–ketone, or polyvinylidene fluoride) or rigid ceramic supports (alumina, silica, zirconia, etc.) are frequently used for the preparation of flat or hollow-fiber membranes. However, polymer support materials typically degrade at elevated temperatures, swell in harsh conditions and suffer from the physical/chemical aging or plasticization [5–8] whereas ceramic supports have some limitations in respect to fragility and

* Corresponding author.
E-mail address: zdenek.sofer@vscht.cz (Z. Sofer).

https://doi.org/10.1016/j.apmt.2019.02.014
2352-9407/

production costs [1,4–6]. In the past decades, the attention of researchers in gas separation area began to focus on the development and engagement of carbon- or graphene-based materials [9–20] due to their versatile and tunable properties enabling to overcome the limitations of polymeric or ceramic materials [1,6,9]. The remarkable position of carbon nanotubes (CNT) was reported by Iijima for the first time [21]. Basically, CNT could be imagined as the hollow seamless cylinders consisting of one or more rolled-up graphene sheets with the planar-hexagonal distribution of carbon atoms in a honeycomb lattice arrangement [21–23]. Based on the number of rolling graphene layers, CNT can be classified as single-walled carbon nanotubes (SWCNT), double-walled carbon nanotubes or multi-walled carbon nanotubes. The properties of CNTs are highly related to their size, diameter, and morphology [16,24,25]. In the field of gas separation, CNT have been recognized as a perfect construction element for fabrication of various kinds of separation membranes such as polymer-based mixed matrix membranes (MMM) [13,16], carbon-CNT composites [26], CNT-inorganic hybrids [27] and other CNT-nanostructured materials [28–30]. Due to unique properties such as excellent electrical and thermal conductivity, high specific surface area, flexibility, the incorporation of CNT into the membrane matrix generally enhanced the mechanical, thermal and chemical resistance and separation performance [13,17].

Furthermore, the inclination of nanotubes to form bundles by agglomeration and the ability to assemble into certain multidirectional networks enabled to form paper-like materials, referred to as buckypaper (BP) [31]. CNT-BP is a self-supported membrane material with entangled CNT forming a physically and chemically stable, flexible structure that offers the advantage of the easy application as permeable membranes, capacitors, electrodes for fuel cells, etc. [31,32]. Due to the porous surface and stronger interfacial adhesion, CNT-BP could be utilized as the interlaminar reinforcement material in hybrid composite membranes [33].

Suitable processing technique of raw CNT followed by assembling into the CNT-BP material is vacuum filtration or sedimentation/drying processes. The arrangement of individual CNT fibers inside of BP has a great influence on the final material properties. BPs were already suggested for membrane gas/liquid separation applications. Kim et al. reported CNT membrane used as support for the ultra-thin graphene oxide separation layer [34]. CNT support with porous structure exhibited excellent chemical stability in various organic solvents while maintaining high flux. In addition, quantum mechanical calculations were performed to show that CNT with porous walls can be efficiently used for separation of H_2/CH_4 and CO_2/CH_4 gas mixtures [35]. Simultaneously, barrier or retention properties of BPs were reported for filtration of aerosol particles [36,37], bacteria [38,39], gold nanoparticles [40] and organic molecules [31,41].

Thus, SWCNT are conclusively the appropriate material for new high-performance support materials development. Since the common supports for composite separation membranes are fabricated with the aim to have minor or negligible influence on the molecular transport, our motivation was to develop new, stable, active high-performance membrane support materials with comparable or higher permeability but with improved selectivity toward H_2/CO_2 gas pair. In this work, we present free-standing ultrapermeable CNT buckypaper membrane material made of mildly oxidized SWCNT with an enhanced separation efficiency toward the H_2/CO_2 gas pair. We assume that gas selective support in composite membrane could contribute positively to the overall separation performance usually determined only by the H_2/CO_2 selectivity of the top layer.

2. Results and discussion

High-quality, Tuball^{TM} SWCNT with a diameter of nanotubes below 2 nm were used for BP preparation. Selected SWCNT represent currently the cheapest available material on the market and many researchers are investigating their properties for applications in polymer composites and purification applications [42–45].

Chemical oxidation of SWCNT was performed by a modified Hummers method utilizing potassium permanganate in an acidic environment. In comparison to the classic Tour or Hummers oxidation procedure [46], a smaller amount of permanganate was used (1/8 of the original dose used in Tour procedure). Oxidation was followed by a purification procedure performed by decantation and filtration until the neutral pH was achieved. Purified SWCNT were then transferred to the distilled water and dispersed using high energy shear-force milling (Ultra Turrax). A prepared stocked water suspension of oxidized SWCNT was stable and do not exhibit any sedimentation even after three months.

BP was obtained from stock dispersion of oxidized SWCNT by simple filtration technique. Using this simple, robust and scalable process, the self-supporting BP membranes with a diameter of 9 cm and the thickness ranging from 200 μm to 1000 μm were prepared. Additionally, BPs from unmodified SWCNT were prepared for comparison.

Scanning electron microscopy (SEM) was used for observation of the oxidized SWCNT based BP surface. As can be seen in Fig. 1A, the membrane structure is composed of agglomerated entangled bundles of individual SWCNT similarly to structures already described in the literature [47]. Membrane exhibits porous structure with the pores formed by free space between entangled SWCNT bundles (pore diameter of several tens of nanometers). Such a highly porous structure is advantageous for high flux membrane applications. In

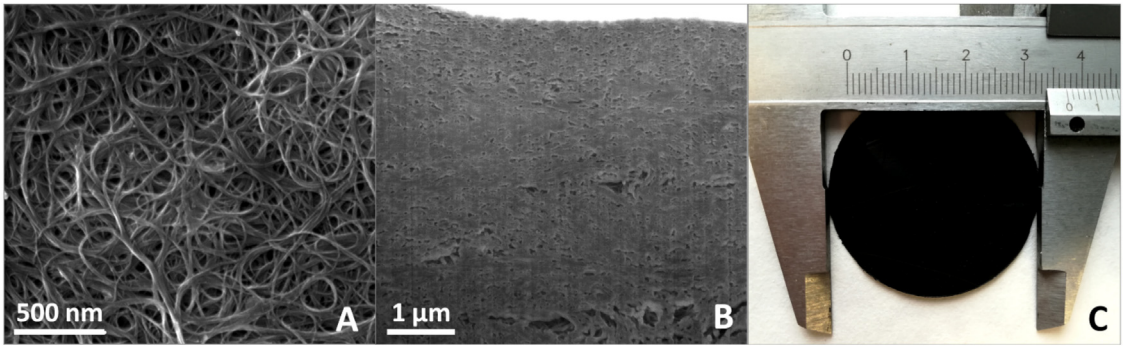

Fig. 1. The morphology of oxidized SWCNT membrane observed from (A) top and (B) cross-section. (C) Optical image of as-prepared freestanding BP prepared from oxidized SWCNT.

Table 1
The chemical composition of bare and oxidized SWCNT obtained from survey XPS spectra and by energy dispersive spectroscopy (EDS) coupled with SEM.

	XPS survey spectra		SEM-EDS	
	Bare	Oxidized	Bare	Oxidized
C (at.%)	93.17	73.33	92.92	85.99
O (at.%)	6.83	21.31	3.03	9.99
S (at.%)	–	5.36	0.17	2.30
C/O	13.64	3.44	30.67	8.61

addition to that, the morphology of membrane in cross-section was also studied. Fig. 1B shows the interconnected pores in the whole width of the cross-section. The porous structure provides a material with the high surface area which can be utilized for interactions of retentate with an inner membrane surface. The chemical composition obtained by energy dispersive spectroscopy (EDS) is shown in Table 1. Optical image of BP prepared using oxidized SWCNT is shown in Fig. 1C.

Influence of oxidation procedure on the SWCNT morphology was studied using atomic force microscopy (AFM), results are shown in Fig. 2. It is evident that even a small amount of $KMnO_4$ in concentrated acid can change dramatically the nanotube morphology. Oxidized nanotubes still exhibit some degree of original tubular character, however, at the same time, they seemed to be more agglomerated. Such behavior can be explained by the hydrogen bonding between adjacent carboxylic groups [48], by the oxidative opening of nanotube ends (tips) or by the creation of holes and cracks [49,50]. The partial opening of nanotubes could be advantageous for separation applications since it makes more surface area accessible for retentate–membrane interactions (open nanotubes expose both inner and outer part to the surrounding environment).

In order to support our hypotheses that mild oxidation leads to opening of nanotube end tips, HR-TEM was used to observe oxidized SWCNT. Even mild oxidation results in damaged SWCNT, mainly its end tips (Fig. 3). End tips seem to be more disordered and corrugated than sidewalls of carbon nanotubes. This observation supports our hypothesis about preferential oxidation of end tips and its subsequent opening.

Raman spectroscopy was used to evaluate the effect of the oxidation procedure on the defects density in SWCNT (Figure SI1). Bare SWCNT exhibit only the G (graphitic) peak at 1585 cm^{-1} which is related to the presence of carbon atoms with the sp^2 hybridization. In general, oxidation procedure results in disruption of the carbon lattice and the introduction of various oxygen functional groups which is accompanied by a change in hybridization state to the sp^3. However, mild oxidation of SWCNT with only 1/8 of permanganate amount originally used in Tour method does not result in an introduction of the D (defect) peak at 1350 cm^{-1} related to sp^3 hybridization. This is an indication of the very mild oxidation state of SWCNT where only ends of SWCNT were most probably functionalized by oxygen moieties. Another possible explanation could be the oxidative elimination of organic/amorphous carbon and metallic impurities. The opening of carbon nanotube should be accompanied by the disappearance of radial breathing mode (RBM) at ~150–300 cm^{-1}; which is not our case since the RBM can be clearly observed even after mild oxidation [51].

Since the Raman spectroscopy was not able to prove any significant changes in the defect density of oxidized SWCNT, further investigation was performed using highly surface sensitive X-ray photoelectron spectroscopy (Fig. 4). Chemical compositions obtained from survey XPS spectra revealed an increase of oxygen concentration in oxidized SWCNT in comparison to the bare one (see Table 1) as indicated by lower C/O ratio. Significantly lower C/O ratio of oxidized SWCNT was further confirmed by other analytical techniques as described below, which proved successful chemical modification. In addition to that, deconvolution of high-resolution XPS spectra of C 1s region was performed in order to get a better understanding of carbon atoms bonding states (see Fig. 4 and Table 2). Its results suggest that most of the carbon atoms still forms a conjugated network even after mild oxidation procedure. Furthermore, it shows an increase in oxygen concentration indicating mild oxidation, especially at the end caps. End caps exhibit the highest reactivity in SWCNT structure due to its higher curvature compared to SWCNT sidewalls. Higher reactivity is caused by the curvature induced strain that originates from pyramidalization of sp^2-hybridized carbon atoms and misalignment of π-orbitals [52]. Additionally, the significant amount of sulfur was detected in oxidized SWCNT which originates from sulfuric acid used during oxidation.

Combustion elemental analysis was performed in order to precisely evaluate the chemical composition of prepared materials

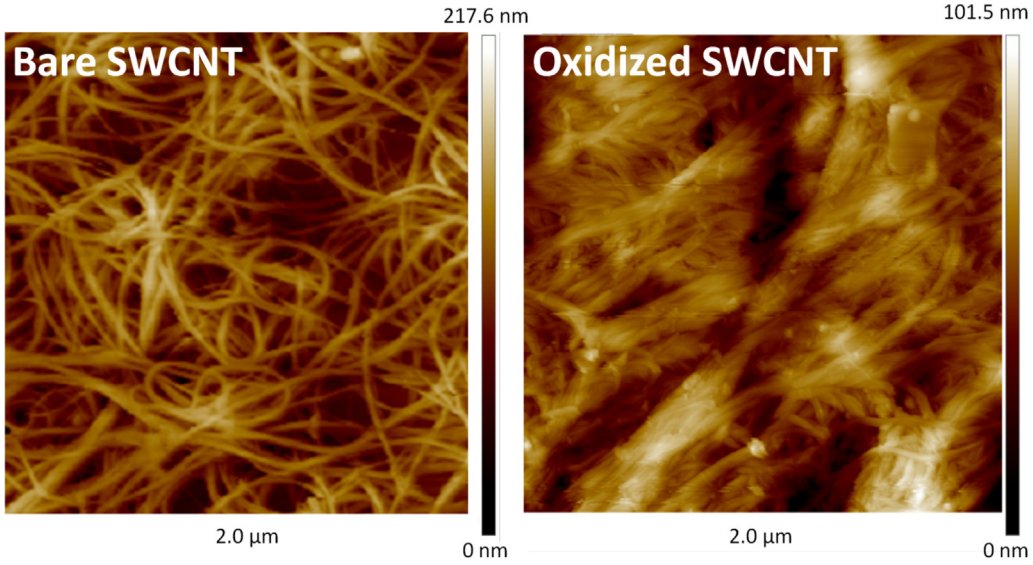

Fig. 2. Morphology of BP made of bare and oxidized SWCNT obtained by AFM.

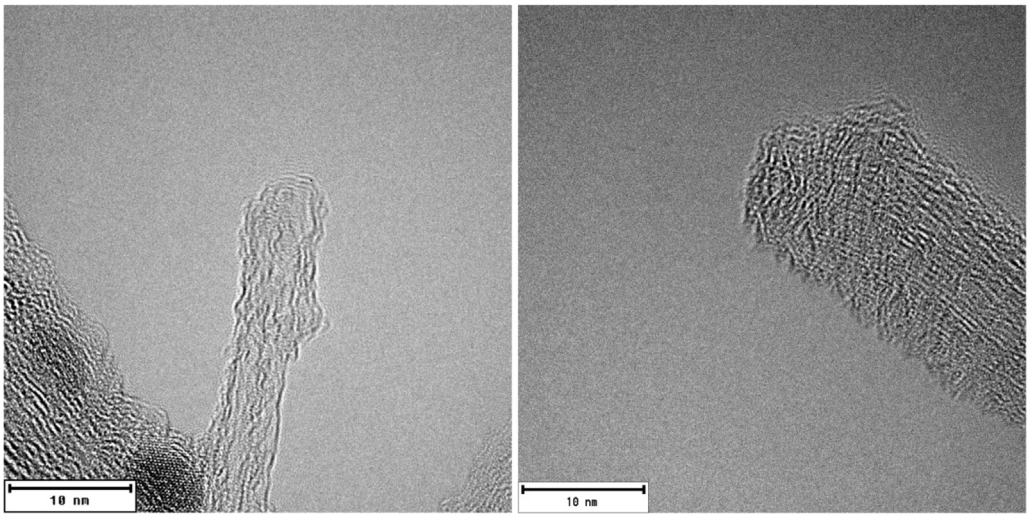

Fig. 3. HR-TEM image of agglomerated oxidized SWCNT end tips showing highly that oxidation damage mainly nanotube end tips.

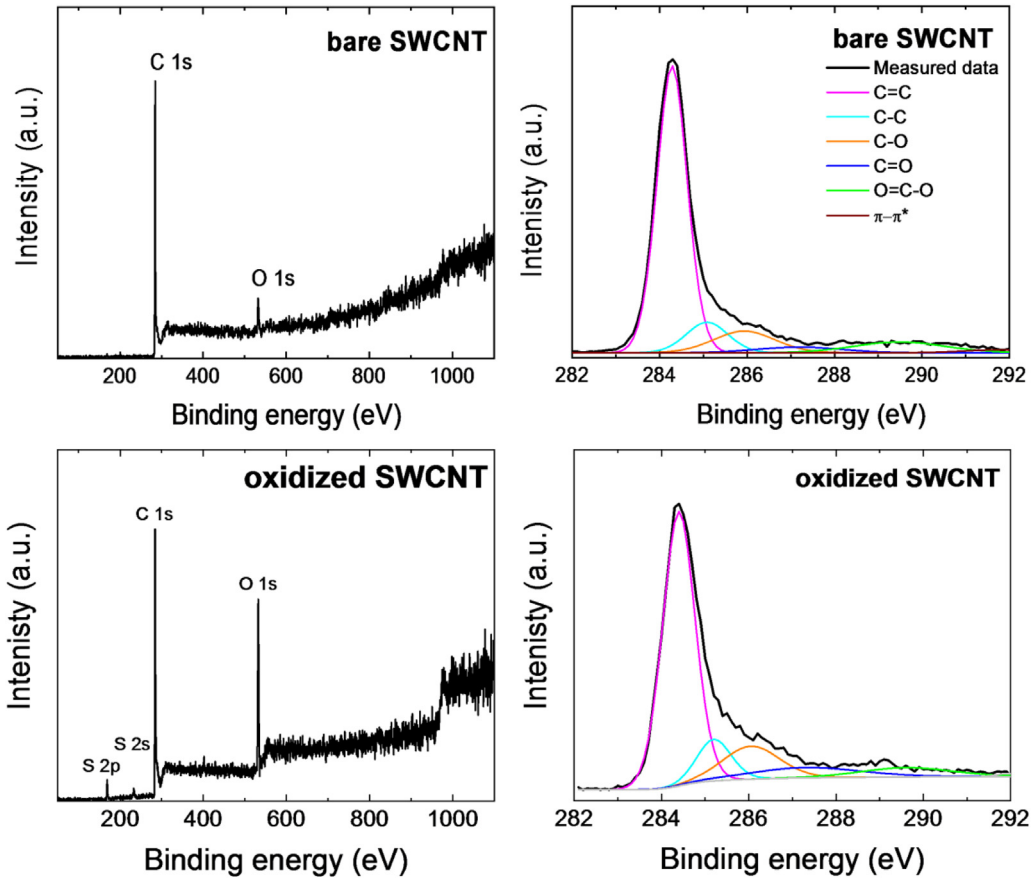

Fig. 4. XPS survey spectra and high-resolution spectra of C1s region of bare and oxidized SWCNT.

(see Table 3). Bare unmodified SWCNT are composed mainly of carbon with oxygen and hydrogen impurities, most likely introduced during synthesis of CNT. Oxidation of SWCNT results in an increase of oxygen concentration (represented by the lower C/O ratio shown in Table 1) as well as hydrogen which suggests successful decoration of SWCNT with oxygen functionalities. As described above, oxidized SWCNT contain some remaining sulfur which originates from sulfuric acid used during oxidation procedure. Lower C/O ratio of modified SWCNT compare to unmodified ones suggest, that even a very low amount of potassium permanganate can be successfully used for mild SWCNT oxidation. The chemical composition obtained by EDS (Table 1) shows a similar trend in element concentrations as XPS results.

Mechanical strength is one of the most important parameters that influence the real-life application of materials for membrane supports. Tensile strength together with ductility of BP made of bare and oxidized SWCNT was evaluated (see Fig. 5). It is clearly obvious that oxidation of SWCNT led to the deterioration of mechanical properties when tensile strength decreases more than the two times. This is most likely caused by the introduction

Table 2
The results of C 1s region deconvolution of bare and oxidized SWCNT.

SWCNT	C=C	C–C	C–O	C=O	O–C=O	π–π^*
Bare	66.84	9.45	9.86	4.28	7.70	1.87
Oxidized	62.35	10.01	13.16	8.07	6.04	0.40

Table 3
The chemical composition of bare and oxidize SWCNT obtained by combustion elemental analysis.

SWCNT	C (at.%)	H (at.%)	N (at.%)	S (at.%)	O (at.%)	C/O
Bare	76.7	12.4	0.07	0	10.8	7.1
Oxidized	53.8	24.1	0.07	2.0	20.0	2.7

of oxygen functionalities. On the other hand, BP prepared from oxidized SWCNT exhibit almost three times higher tensile ductility. Thus, the BP made of oxidized SWCNT can undergo significant plastic deformation before the rupturing occurs. High ductility of BP is advantageous in membrane application since the plastic deformation can easily compensate for the pressure applied to the membrane. Presented values were determined as an average of five individual measurements.

In addition to that, the dynamical mechanical analysis was performed in order to assess the behavior of BP material under elevated temperatures (Figure SI2). As the temperature increases the complex modulus (E^*) and storage modulus (E') increase slightly up to 90 °C. This is most likely related to the thermal ability of oxygen functionalities. Above 100 °C, the moduli decrease moderately due to material softening. Nevertheless, the moduli values lay within a small range of 130 and 160 MPa. The loss factor (tan delta) shows the opposite trend to the complex or storage moduli, varying in the narrow range of 0.13–0.17 and showing no transition temperature. The loss modulus (E'') is almost independent on the temperature. Thus, the dynamic mechanical properties are stable in the whole temperature range under consideration (20–200 °C), which is advantageous for prospective application as membrane supports.

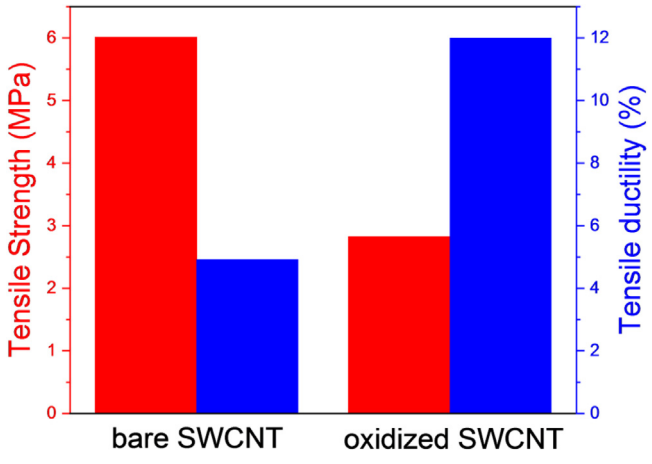

Fig. 5. Tensile strength and ductility of BP prepared form bare and oxidized SWCNT.

Furthermore, the gas permeability of SWCNT samples for hydrogen and carbon dioxide were tested. The used time-lag technique was the same as for previously reported graphene oxide (GO) self-standing 20 μm films [53] created from highly oxidized graphite. Table 4 summarized our results and provides a comparison of the separation performance of various other membranes based on CNT. However, it has to be mentioned that membranes used for comparison in Table 4 exhibit totally different structure compared to our material. Furthermore, there is much more published work related to the membrane for separation of H_2/CO_2 gas mixture which, however, cannot be compared to our material due to the missing information (CO_2 permeance, thickness, etc.) [54–57]. Permeance of oxidized SWCNT membrane reached extraordinary high values compared to other membranes in literature. We believe that the novelty of our work is in preparation of membrane support material with extremely high permeance and good selectivity of H_2/CO_2 gas mixture (3.6). Incorporation of the thin top selective layer could bring membrane materials with interesting separation performance.

In carbon-based membrane materials, the molecular sieving (activated diffusion), the surface diffusion (selective adsorption), the Knudsen diffusion, and the viscous (Poiseuille) flow are the generally accepted mechanisms [9,11,17,29,60]. The contribution of each mechanism to the gas transport is dependent on the membrane material properties (i.e. pore size and the pore size distribution, composition), the nature of permeating gases (thermodynamic properties, interaction with the membrane material) and the operating conditions (temperature and pressure) as well. The molecular sieving is the predominant transport mechanism when the membrane pores similar to molecular dimensions of the diffusive gas. The surface diffusion transport mechanism occurs when permeate gas exhibits a strong affinity for the membrane surface and gas molecules are prevailingly adsorbed along the pore walls. Knudsen diffusion mechanism takes place along narrow pores where the collision of molecules to the pore walls is more frequent than the collision between individual molecules. The separation selectivity is proportional to the inverse ratio of the square root of the molecular weights, i.e. 4.7 for the H_2/CO_2 [9,60]. The viscous flow mechanism is dominant for highly permeable and low selective membranes where the molecular transport takes place through pores with a diameter larger than 20 nm [9,60].

In the case of H_2/CO_2 gas pair separation, two opposing factors affect the entire separation process. The difference in molecular size between H_2 and CO_2 (kinetic diameter H_2: 2.89 Å versus CO_2: 3.30 Å) [13] is manifested by larger hydrogen diffusivity and permeability, respectively compared to CO_2. And vice versa, the difference in critical temperature (CO_2: 304 K versus H_2: 33 K) [17] implies easier CO_2 condensability and thus much higher CO_2 solubility inside membrane relative to H_2. In our case, the effect of mild SWCNT oxidation on gas permeability and selectivity is evident. In bare form, both gas permeability is almost identical due to the macroscopic-size volume elements among the assembled nanotubes. Therefore, bare SWCNT material is extremely permeable due

Table 4
Results of gas permeability and corresponding H_2/CO_2 selectivity. In third column should be Permeance, P (GPU)a CO2

Sample	Permeance, P(GPU)[a] H_2	CO_2	Ideal selectivity α (P_{H2}/P_{CO2})(–)
Bare SWCNT (this work)	31 907	29 225	1.1
Oxidized SWCNT (this work)	33 601	9674	3.5
GO [53]	123	35	3.6
RA-CNT [58]	2510	997	2.5
PA-CNT [58]	985	203	4.9
CoAPO-5/PS/CNT [59]	836	137	6.1

[a] 1 GPU = 3.35×10^{-10} mol m^{-2} s^{-1} Pa^{-1}.

to a dominant viscous flow transport mechanism but completely not selective for light gases. Contrarywise, in case of the oxidized form, a partial opening of the nanotubes (confirmed by AFM) most likely created the additional obstacles for the molecular transport, reduced the unoccupied (free) volume among nanotubes and thus reduced the overall permeability of SWCNT material. Simultaneously, the presence of protruding oxygen-containing species in oxidized SWCNT samples (confirmed by elemental analysis and EDS), that potentially can hinder gas molecules by it is own electron density, non-covalent interaction between fibers and/or via interactions with CO_2 penetrating molecules, contributed to a reduction in H_2 and CO_2 gas permeability too. An observed substantial drop in gas permeability (circa 4.5 times for H_2 and 14 times for CO_2 compared to bare form) is compensated by increased separation efficiency toward the H_2/CO_2 gas pair equaled to 3.5 while non-selective bare sample has 1.1 only. The transport mechanism in oxidized SWCNT samples is presumably predominantly driven by the viscous flow, but with regard to the increase in the selectivity value, there are, in a limited way, the contributions of other mechanisms presented as well. Potentially, inverse gas chromatography could be utilized to get better insight into the separation mechanism that takes place in our membrane [61]. In comparison with our previously reported permeability and selectivity of graphene oxide film overcoming the benchmarking H_2/CO_2 Robeson upper bound [62], a selectivity of oxidized SWCNT is reaching almost the same value like GO (3.6) [53] but exceeds it by three orders of magnitude higher gas permeabilities compared to GO film.

3. Conclusion

We demonstrated that the concept of the mild oxidation of the single-wall carbon nanotubes with only 1/8 of potassium permanganate of the classic Tour method dose is suitable for the preparation of mildly functionalized SWCNT. Further, flat buckypaper membranes based on bare and oxidized SWCNT were prepared by a simple vacuum filtration method and tested as potential membrane support materials usable for efficient H_2/CO_2 separation membranes. It was demonstrated that the mild oxidation affects specifically the properties of SWCNT and that re-arranged, modified structure of the nanotubes exhibited both suitable mechanical and gas permeability-selectivity properties. The proven ability of oxidized SWCNT to actively separate H_2 and CO_2 gases makes these materials potentially attractive as a support for the high-performance hybrid or composite membranes for effective hydrogen separation. The remaining challenge for near future lies in the preparation of operational highly permeable composite SWCNT-based membranes with a top skin layer from the highly H_2/CO_2 selective polymer. We believe that active support materials could bring a radical improvement in the preparation of highly efficient gas separation membranes with a performance level close to the 2008 Robeson upper bound or completely behind it.

4. Experimental

4.1. Materials

TUBALL™ single-wall carbon nanotubes (metal impurities 15 wt.%, diameter 1.8 nm, length 5 μm) were obtained from OCSiAl. Sulphuric acid (96 wt.%), phosphoric acid (85 wt.%), potassium permanganate, hydrogen peroxide (25 wt.%) were obtained from Penta, Czech Republic. Hydrogen and carbon dioxide with purity of 99.9995% (5.5) and 99.990% (4.0), respectively were supplied by SIAD ČR s.r.o., the Czech Republic.

4.2. SWCNT oxidation

Concentrated sulfuric acid (900 ml) and phosphoric acid (120 ml) were mixed in the beaker and cooled in the refrigerator. Then, single wall carbon nanotubes (3 g) were added and properly mixed into the solution using a Teflon anchor stirrer. Potassium permanganate (0.2 g) was added in small portion during the period of 5 min. The reaction temperature was kept below 50 °C using an ice bath. When all permanganate was added the reaction mixture was stirred for another 2 h. Finally, the suspension was poured into the mixture of ice and water (2 l) and unreacted permanganate was decomposed by hydrogen peroxide. Sulfuric acid was removed by repeated decantation and filtration till neutral pH was reached. The final product was mixed with water (0.1 wt.%) and stir by ULTRA-TURRAX® disperser for 1 h at 10 000 rpm. This dispersion was once more filtrated and the final water dispersion was stored for the next usage.

4.3. Membrane preparation

According to the thickness of the membrane, the desired volume of oxidized SWCNT water dispersion was poured onto Büchner funnel with a nylon membrane filter (diameter 47 mm, pore size 0.45 μm), filtrate under vacuum and washed with water and ethanol. Solid self-standing buckypaper was put between two waxed papers and glass, weight down and dried at a temperature of 60 °C. Afterward, dried membranes were stored at ambient conditions before further use.

4.4. Single gas permeability measurements

Single gas permeation experiments were carried out using the fixed-volume pressure-increase apparatus [63,64] at 25 °C and atmospheric pressure. A sample membrane (the active area of 2.01 cm^2) was supported with a sintered steel plate, sealed with an NBR flat O-ring. The permeation of gas into the fixed-volume (permeate) chamber was followed using a pressure gauge (Leybold Ceravac CTR 100 N) with maximum permeation pressure of 1333 mbar.

The permeability coefficients were calculated from steady-state regions as [63,64]:

$$P = \frac{V}{A \cdot R \cdot T} \cdot \frac{l}{p_{atm}} \cdot \frac{dp}{dt} \quad (1)$$

in which dp/dt is the slope of the pressure increase in the fixed-volume permeate chamber under steady-state conditions, A is the active area of the membrane and l is the membrane thickness.

4.5. Analytical techniques

The morphology was investigated via scanning electron microscopy (SEM) using a FEG electron source (Tescan Lyra dual beam microscope). To conduct these measurements, the samples were placed on a carbon conductive tape. SEM and SEM-EDS measurements were carried out using a 10 kV electron beam. The chamber pressure was 1×10^{-3} Pa and the working distance was 5 mm.

High-resolution X-ray photoelectron spectroscopy (XPS) was performed using an ESCAProbeP spectrometer (Omicron Nanotechnology Ltd., Germany) with a monochromatic aluminum X-ray radiation source (1486.7 eV). The samples were placed on a conductive carbon tape homogeneously covered with the sample.

Raman spectroscopy was conducted using an inVia Raman microscope (Renishaw, England) with a CCD detector in backscattering geometry. A DPSS laser (532 nm, 50 mW) with a 100× magnification objective was used for the Raman measurements.

The instrument was calibrated using a silicon reference to give a peak position at 520 cm^{-1} and a resolution of fewer than 1 cm^{-1}.

Combustible elemental analysis (EA) was performed using a PE 2400 Series II CHNS/O Analyzer (Perkin Elmer, USA). The instrument was used in the CHN operating mode (the most robust and interference-free mode) to convert the sample elements to simple gases (CO_2, H_2O, SO_2 and N_2). The PE 2400 analyzer automatically performed combustion, reduction, homogenization of product gases, separation and detection. An MX5 microbalance (Mettler Toledo) was used for precise weighing of the samples (1.5–2.5 mg per single sample analysis). Using this procedure, the accuracy of CHN determination is better than 0.30% abs. Internal calibration was performed using N-phenyl urea.

The dynamic mechanical analysis was measured on DMA DX04T (by RMI, Czech Republic). A sample with dimensions 7.600 mm (width), 0.173 mm (thickness) and 10.200 mm (active length) was loaded with a tensile longitudinal sinusoidal deformation with the amplitude of 0.02 mm and pre-tension of 0.03 mm. The temperature range was 20–200 °C with a heating rate of 2 °C min^{-1} in the air atmosphere. From the results, the values of moduli and loss factor were evaluated as the second order sliding average.

Characterization by Atomic Force Microscopy (AFM) was performed on NT-MDT Ntegra Spectra (NT-MDT) in tapping mode. Before the measurement, samples were diluted in isopropyl alcohol (0.1 mg mL^{-1}), sonicated for 5 min and drop cast on a freshly cleaved mica substrate.

Acknowledgments

This project (TH03020348) was supported by Technology Agency of the Czech Republic (TAČR, program Epsilon), by the Czech Science Foundation (GAČR No. 17-05421S acknowledged by K.F.) and by specific university research (MSMT SVV-20/2018). This work was supported by the project Advanced Functional Nanorobots (reg. No. CZ.02.1.01/0.0/0.0/15_003/0000444 financed by the EFRR).

Appendix A. Supplementary data

Supplementary data associated with this article can be found, in the online version, at doi:10.1016/j.apmt.2019.02.014.

References

[1] Z. Dai, L. Ansaloni, L. Deng, Recent advances in multi-layer composite polymeric membranes for CO_2 separation: a review, GEE 1 (2016) 102–128.
[2] S.X. Leong, M. Carta, R. Malpass-Evans, N.B. McKeown, E. Madrid, F. Marken, One-step preparation of microporous Pd@ cPIM composite catalyst film for triphasic electrocatalysis, Electrochem. Commun. 86 (2018) 17–20.
[3] Y. Yin, M.D. Guiver, Microporous polymers: ultrapermeable membranes, Nat. Mater. 16 (2017) 880.
[4] E. Pinnau, Membrane separations, in: I.D. Wilson (Ed.), Encyclopedia of Separation Science, Academic Press, 2000, pp. 1755–1764.
[5] M. Freemantle, Membranes for gas separation, Chem. Engin. News 83 (2005) 49–57.
[6] P. Bernardo, E. Drioli, G. Golemme, Membrane gas separation: a review/state of the art, Ind. Eng. Chem. Res. 48 (2009) 4638–4663.
[7] N.B. McKeown, A perfect match, Nat. Mater. 17 (2018) 216–217.
[8] Z.P. Smith, D.F. Sanders, C.P. Ribeiro, R. Guo, B.D. Freeman, D.R. Paul, J.E. McGrath, S. Swinnea, Gas sorption and characterization of thermally rearranged polyimides based on 3,3′-dihydroxy-4,4′-diamino-biphenyl (HAB) and 2,2′-bis-(3,4-dicarboxyphenyl) hexafluoropropane dianhydride (6FDA), J. Membr. Sci. 415 (2012) 558–567.
[9] J.B.S. Hamm, A. Ambrosi, J.G. Griebeler, N.R. Marcilio, I.C. Tessaro, L.D. Pollo, Recent advances in the development of supported carbon membranes for gas separation, Int. J. Hydrogen Energ. 42 (2017) 24830–24845.
[10] W.N.W. Salleh, A.F. Ismail, Preparation of carbon membranes for gas separation, in: E. Drioli, L. Giorno, E. Fontananova (Eds.), Comprehensive Membrane Science and Engineering, 2nd ed., Elsevier, 2017, pp. 330–357.
[11] N. Song, X. Gao, Z. Mac, S. Wanga, Y. Wei, C. Gao, A review of graphene-based separation membrane: materials, characteristics, preparation and applications, Desalin 437 (2018) 59–72.
[12] L. Li, C. Song, D. Jiang, T. Wang, Preparation and enhanced gas separation performance of carbon/carbon nanotubes (C/CNTs) hybrid membranes, Separ. Purif. Tech. 188 (2017) 73–80.
[13] M. Vinoba, M. Bhagiyalakshmi, Y. Alqaheem, A.A. Alomair, A. Pérez, M.S. Rana, Recent progress of fillers in mixed matrix membranes for CO_2 separation: a review, Sep. Pur. Technol. 188 (2017) 431–450.
[14] D. Bouša, K. Friess, K. Pilnáček, O. Vopička, M. Lanč, K. Fónod, M. Pumera, D. Sedmidubsky, J. Luxa, Z. Sofer, Thin, high-flux, self-standing, graphene oxide membranes for efficient hydrogen separation from gas mixtures, Chem. Eur. J. 23 (2017) 11416–11422.
[15] C. Chi, X. Wang, Y. Peng, Y. Qian, Z. Hu, J. Dong, D. Zhao, Facile preparation of graphene oxide membranes for gas separation, Chem. Mater. 28 (2016) 2921–2927.
[16] M.N. Nejad, M. Asghari, M. Afsari, Investigation of carbon nanotubes in mixed matrix membranes for gas separation: a review, Chem. Bio. Eng. Rev. 3 (2016) 276–298.
[17] S.S. Swain, L. Unnikrishnan, S. Mohanty, S.K. Nayak, Carbon nanotubes as a potential candidate for separation of H_2–CO_2 gas pairs (review article), Int. J. Hydrog. Energ. 42 (2017) 29283–29299.
[18] M. Rashid, S.F. Ralph, Carbon nanotube membranes: synthesis, properties, and future filtration applications, Nanomaterials 7 (2017) 99–127.
[19] E.F. Belin, Characterization methods of carbon nanotubes: a review, Mat. Sci. Eng. B 119 (2005) 105–118.
[20] P. Calvert, Nanotube composites: a recipe for strength, Nature 399 (1999) 210.
[21] S. Iijima, Helical microtubules of graphitic carbon, Nature 354 (1991) 56–58.
[22] J. Prasek, J. Drbohlavova, J. Chomoucka, J. Hubalek, O. Jasek, V. Adam, R. Kizek, Methods for carbon nanotube synthesis – review, J. Mater. Chem. B 40 (2011) 15872–15884.
[23] O.A. Aberefa, M.O. Daramola, S.E. Iyuke, Production and functionalization of carbon nanotubes for application in membrane synthesis for natural gas separation, Micropor. Mesopor. Mater. (2019), in press.
[24] B.J. Hinds, N. Chopra, T. Rantell, R. Andrews, V. Gavalas, L.G. Bachas, Aligned multiwalled carbon nanotube membranes, Science 303 (2004) 62–65.
[25] C. Eun, Effect of surface curvature on diffusion-limited reactions on a curved surface, J. Chem. Phys. 147 (2017) 184112.
[26] L. Li, C. Song, D. Jiang, T. Wang, Preparation and enhanced gas separation performance of Carbon/Carbon nanotubes (C/CNTs) hybrid membranes, Sep. Purif. Technol. 188 (2017) 73–80.
[27] P.S. Lee, D. Kim, S.E. Nam, R.R. Bhave, Carbon molecular sieve membranes on porous composite tubular supports for high performance gas separations, Micropor. Mesopor. Mater. 224 (2016) 332–338.
[28] Q.S. Yang, X.Q. He, X. Liu, F.F. Leng, Y.W. Mai, The effective properties and local aggregation effect of CNT/SMP composites, Comp. B Eng. 43 (2012) 33–38.
[29] W.N.W. Salleh, A.F. Ismail, Carbon membranes for gas separation processes: recent progress and future perspective, J. Membr. Sci. Res. 1 (2015) 2–15.
[30] U. Narayan-Maiti, Chemically modified/doped carbon nanotubes & graphene for optimized nanostructures & nanodevices, Adv. Mater. 26 (2014) 40–67.
[31] X. Yang, J. Lee, L. Yuan, S.R. Chae, V.K. Peterson, A.I. Minett, Y. Yin, A.T. Harris, Removal of natural organic matter in water using functionalised carbon nanotube buckypaper, Carbon 59 (2013) 160–166.
[32] J. Rodrigues, D. Mata, A. Pimentel, D. Nunes, R. Martins, E. Fortunato, A.J. Neves, T. Monteiro, F.M. Costa, One-step synthesis of ZnO decorated CNT buckypaper composites and their optical and electrical properties, Mater. Sci. Eng. B 195 (2015) 38–44.
[33] N. Li, G.D. Wang, S.K. Melly, T. Peng, Y.C. Li, Q.D. Zhao, S.D. Ji, Interlaminar properties of GFRP laminates toughened by CNTs buckypaper interlayer, Compos. Struct. 208 (2019) 13–22.
[34] S.J. Kim, D.W. Kim, K.M. Cho, K.M. Kang, J. Choi, D. Kim, H.T. Jung, Ultrathin graphene oxide membranes on freestanding carbon nanotube supports for enhanced selective permeation in organic solvents, Sci. Rep. 8 (2018) 1959.
[35] B.J. Bucior, D.L. Chen, J. Liu, J.K. Johnson, Porous carbon nanotube membranes for separation of H_2/CH_4 and CO_2/CH_4 mixtures, J. Phys. Chem. C 116 (2012) 25904–25910.
[36] G. Viswanathan, D.B. Kane, P.J. Lipowicz, High efficiency fine particulate filtration using carbon nanotube coatings, Adv. Mater. 16 (2004) 2045–2049.
[37] Y. Zhao, Z. Zhong, Z.X. Low, Z. Yao, A multifunctional multi-walled carbon nanotubes/ceramic membrane composite filter for air purification, RSC Adv. 5 (2015) 91951–91959.
[38] A.S. Brady-Estévez, M.H. Schnoor, S. Kang, M. Elimelech, SWNT–MWNT hybrid filter attains high viral removal and bacterial inactivation, Langmuir 26 (2010) 19153–19158.
[39] A.S. Brady-Estévez, S. Kang, M. Elimelech, single-walled-carbon-nanotube filter for removal of viral and bacterial pathogens, Small 4 (2008) 481–484.
[40] S. Roy, V. Jain, R. Bajpai, P. Ghosh, A. Pente, B. Singh, D. Misra, Formation of carbon nanotube bucky paper and feasibility study for filtration at the nano and molecular scale, J. Phys. Chem. C 116 (2012) 19025–19031.
[41] J.H. Choi, J. Jegal, W.N. Kim, H.S. Choi, Incorporation of multiwalled carbon nanotubes into poly (vinyl alcohol) membranes for use in the pervaporation of water/ethanol mixtures, J. Appl. Polym. Sci. 111 (2009) 2186–2193.
[42] A.J. Clancy, H.H. Tay, Ch. Yau, M.S.P. Shaffer, Carbon (2016) 423.
[43] A.P.I. Chortos, P. Lin, G. Pitner, X. Yan, T.Z. Gao, J.W.F. To, T. Lei, J.W. Will, H.-S.P. Wong, Z. Bao, ASC Nano (2017) 5660.
[44] B.P.M. Krause, E. Ilin, P. Pötschke, Lyon, AIP Conference Proceedings 1914 030008 (2017), Lyon.
[45] B.P.P. Krause, E. Ilin, M. Predtechenskiy, Polymer (2016) 45.

[46] D.C. Marcano, K.D.V. Berlin, J.M. Sinitskii, A. Sun, A. Slesarev, L.B. Alemany, W. Lu, J.M. Tour, ACS Nano (2010) 4806.
[47] Y.A. Kim, H. Muramatsu, T. Hayashi, M. Endo, M. Terrones, M.S. Dresselhaus, Fabrication of high-purity, double-walled carbon nanotube buckypaper, Chem. Vap. Deposition 12 (2006) 327–330.
[48] A.K. Nair, Z. Qin, M.J. Buehler, Cooperative deformation of carboxyl groups in functionalized carbon nanotubes, Int. J. Solid Struct. 49 (2012) 2418–2423.
[49] Y.-S. Li, J.-L. Liao, S.-Y. Wang, W.-H. Chiang, Intercalation-assisted longitudinal unzipping of carbon nanotubes for green and scalable synthesis of graphene nanoribbons, Sci. Rep. 6 (2016) 22755.
[50] S. Tsang, P. Harris, M. Green, Thinning and opening of carbon nanotubes by oxidation using carbon dioxide, Nature 362 (1993) 520.
[51] R. Saito, M. Hofmann, G. Dresselhaus, A. Jorio, M. Dresselhaus, Raman spectroscopy of graphene and carbon nanotubes, Adv. Phys. 60 (2011) 413–550.
[52] N. Karousis, N. Tagmatarchis, D. Tasis, Current progress on the chemical modification of carbon nanotubes, Chem. Rev. 110 (2010) 5366–5397.
[53] D. Bouša, K. Friess, K. Pilnáček, O. Vopička, M. Lanč, K. Fónod, M. Pumera, D. Sedmidubský, J. Luxa, Z. Sofer, Chem. Eur. J. 23 (2017) 11416–11422.
[54] A. Sharma, S. Kumar, B. Tripathi, M. Singh, Y. Vijay, Aligned CNT/polymer nanocomposite membranes for hydrogen separation, Int. J. Hydrog. Energy 34 (2009) 3977–3982.
[55] A. Sharma, B. Tripathi, Y. Vijay, Dramatic improvement in properties of magnetically aligned CNT/polymer nanocomposites, J. Membr. Sci. 361 (2010) 89–95.
[56] S. Kumar, A. Sharma, B. Tripathi, S. Srivastava, S. Agrawal, M. Singh, K. Awasthi, Y. Vijay, Enhancement of hydrogen gas permeability in electrically aligned MWCNT–PMMA composite membranes, Micron 41 (2010) 909–914.
[57] A. Sharma, Y. Vijay, Effect of electric field variation in alignment of SWNT/PC nanocomposites, Int. J. Hydrog. Energ. 37 (2012) 3945–3948.
[58] B. Kueh, M. Kapsi, C.M. Veziri, C. Athanasekou, G. Pilatos, K.S.K. Reddy, A. Raj, G.N. Karanikolos, Asphaltene-derived activated carbon and carbon nanotube membranes for CO_2 separation, Energy Fuels 32 (2018) 11718–11730.
[59] A. Labropoulos, C. Veziri, M. Kapsi, G. Pilatos, V. Likodimos, M. Tsapatsis, N.K. Kanellopoulos, G.E. Romanos, G.N. Karanikolos, Carbon nanotube selective membranes with subnanometer, vertically aligned pores, and enhanced gas transport properties, Chem. Mater. 27 (2015) 8198–8210.
[60] A.F. Ismail, D. Rana, T. Matsuura, H.C. Foley, Transport mechanism of carbon membranes, in: Carbon-based Membrane Separation Process, Springer Science & Business Media, 2011, pp. 5–16.
[61] L. Lapčík, M. Otyepka, E. Otyepková, B. Lapčíková, R. Gabriel, A. Gavenda, B. Prudilová, Surface heterogeneity: information from inverse gas chromatography and application to model pharmaceutical substances, Curr. Opin. Colloid Interface Sci. 24 (2016) 64–71.
[62] L.M. Robeson, The upper bound revisited, J. Membr. Sci. 320 (2008) 390–400.
[63] K. Friess, P. Sysel, E. Minko, M. Hauf, O. Vopička, V. Hynek, K. Pilnáček, M. Šípek, Comparison of transport properties of hyperbranched and linear polyimides, Desalin. Water Treat. 14 (2010) 165–169.
[64] P. Sysel, E. Minko, M. Hauf, K. Friess, V. Hynek, O. Vopicka, K. Pilnacek, M. Sipek, Mixed matrix membranes based on hyperbranched polyimide and mesoporous silica for gas separation, Desalin. Water Treat. 34 (2011) 211–215.